

Gasoline Direct Injection Engine Injector Tip Drying

N. Karwa^{1,2}, P. Stephan¹, W. Wiese³, D. Lejsek³

¹Institute of Technical Thermodynamics / Center of Smart Interfaces
Technische Universität Darmstadt, Darmstadt 64287, Germany

²School of Aerospace, Mechanical and Manufacturing Engineering,
RMIT University, Melbourne 3000, Australia

³Robert Bosch GmbH, 70442 Stuttgart, Germany

Abstract

In gasoline direct injection (GDI) engines, carbonaceous deposits are formed on surfaces wetted with gasoline. Of particular concern is the formation of carbonaceous deposits on the injector tip as they lead to injector plugging and particulate emissions from these engines. The drying of the injector tip is an essential parameter in the build-up of deposits. This paper reports the effect of parameters such as system pressure, injector tip temperature and air flow on the drying rate of an isoctane thin film on an injector tip. Depending on the injector tip superheat, the fuel film drying out process can be dominated by either evaporation or boiling. At injector tip superheat up to 10 °C, evaporation at the contact line is the dominating mechanism. The drying rate in this regime increases with injector tip temperature and air velocity. Above this temperature, bubbles or funnel-shaped structures were formed in the film. The drying rate due to boiling depends on the system pressure and temperature but shows little dependence on the air velocity. The drying rate increases with the reduction in system pressure. In the Leidenfrost state, the fuel bounces-off the injector tip and this temperature decreases with system pressure.

Introduction

Similar to that in a diesel engine, albeit at a much lower injection pressure, fuel is injected directly into the combustion chamber during the intake stroke in a gasoline direct injection engine (GDI). This injection strategy offers precise control on the injection timing and fuel dispensing as compared to multiport fuel injection, which results in better fuel economy. However, these engines have higher particle emissions mainly due to less homogenous fuel air mixture within the combustion chamber [8]. The limited fuel air mixing leads to wet combustion chamber, valves, piston, injector and spark plug. Carbonaceous deposits are formed on surfaces wetted with gasoline over a period of engine operation [7]. Of particular concern is the formation of carbonaceous deposits on the injector tip as they lead to injector plugging. Injector plugging is believed to result in power loss and increased emissions [5]. Furthermore, the Euro 6c norm will introduce a particulate number limit for GDI engines and present GDI engines do not meet these limits [1]. Optical investigations inside the combustion chamber of an engine suggest that diffusive combustion of residual film remaining on the injector tip late in the combustion cycle (luminous flame, which suggests a rich fuel-air mixture) is related to the particulate emission [1]. Engine studies have reported that the deposit formation on the injector tip is dependent on a various factors such as injector tip temperature and protrusion into the combustion chamber, composition of the fuel, coating/plating of the tip, etc. [5]. Likely reasons for the change in deposition behaviour could be the change in surface wettability (factors such as fuel composition and tip coatings) or drying rate (factors such as fuel volatility, tip

temperature, and air temperature and velocity). Zhao [12] argued that ensuring the continued presence of liquid fuel on the injector tip during the complete engine cycle would result in the washing away of the deposit precursors during the following injection event. The major constituents of commercial gasoline are saturated alkanes (~70% v/v; octane and isoctane) and aromatics (~25% v/v; Toluene and xylene). Due to their higher boiling temperature as compared to alkanes, aromatics are more likely responsible for deposit formation [11]. In the present study, injector tip drying studies are performed using isoctane as it is representative of the alkane fraction in unleaded gasoline. The objective of the present study is to perform an injector tip drying experiment and determine the effect of parameters such as system pressure, injector tip temperature and air flow on the drying rate. Since it is not possible to recreate realistic in-cylinder conditions in the laboratory, generic experimental studies are performed in a test setup that allows closer control on the varied parameters.

Experimental Methodology

The layout of the experimental set-up is shown in figure 1. The major components of the experimental set-up are: a needle valve for flow regulation, one-way solenoid valve, a 1.5 mm channel including the instrumented test-section at its one end, a vacuum vessel and a vacuum pump. The vacuum pump sets the desired vacuum level in the test section. On opening the solenoid valve, air flows into the channel (20 × 20 mm² cross-section). The flow rate is varied using the needle valve. A smooth channel length of 1.1 m before the test-section ensures an undisturbed fully developed flow in the test section. To allow experiments with higher air flow velocities without appreciable rise in the test section pressure, a vacuum vessel has been installed after the test section. A schematic of the test section is shown in figure 2. A Pitot tube (only a dynamic probe with 1 mm inner diameter) and a static pressure tapping in the channel wall, in conjugation with an ultra-low differential pressure sensor (Sensirion SDP1000-L05: 0.5–125 Pa, 1.5 % of measured value) is used to measure the center line air velocity in the channel. The absolute pressure and temperature in the test section is measured using a pressure sensor (0–1 bar absolute, 0.6 % of full scale) and a 0.5 mm thermocouple, respectively. The injector tip (HDEV5), on which fuel drying studies are to be performed, has been soldered on top of a heating probe constructed from copper. A 1/8" diameter cartridge heater of 35 W rating is embedded into this heating probe. A 0.5 mm diameter thermocouple is embedded in the injector tip to measure its temperature whose output is used by a feed-back controller to regulate the power input to the cartridge heater for maintaining the desired injector tip temperature. The probe is assembled in the test section such that the upward-facing flat face of the injector tip is aligned with the center of the channel (same level as that of Pitot tube's dynamics pressure probe). Fuel is dispensed on the upward-facing surface of the injector tip using a micro-dosing pump. A schematic of the fuel

dispensing is shown in figure 3. The micro-dosing pump (HNP micro annular gear pump m2r-4622 with S-ND controller, smallest dosage volume of 2 μ l) pushes 5 μ l (3.44 mg) isooctane through a 0.3 mm inner diameter needle and the total dispensing duration is about 85 ms. Simultaneous to the injection event, the drying process is recorded using a high-speed long-wave infrared camera (FLIR Orion SC7300L, spectral band of 7.7–9.3 μ m). To allow optical access for the infrared imaging, a ZnSe window is assembled in the channel's top wall. The infrared camera is equipped with a microscopic lens and the field of view is 9.6 \times 7.7 mm². The drying event is recorded at rates of up to 200 frame/s with a resolution of 320 \times 256 pixel². In the experiments done to determine the effect of air flow on the drying rate, the air flow was started just after the end of the fuel dispensing event.

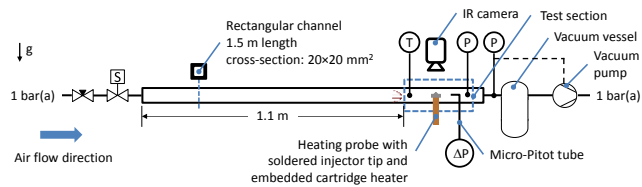


Figure 1. Layout of the experimental set-up.

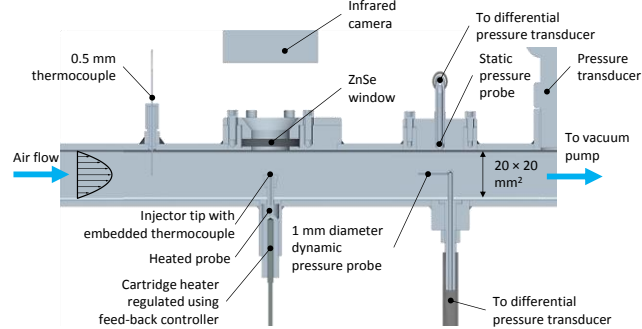


Figure 2. Longitudinal section of the test section.

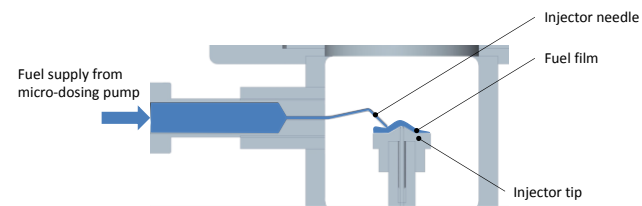


Figure 3. Schematic of the fuel dispensing process.

The experimental parameters for the present are given in Table 1. The typical injector tip temperature is in the range of 120–180 $^{\circ}$ C, increasing with engine load [3]. At start up, the injector might be much cooler; therefore, the test range is between 60 to 170 $^{\circ}$ C. The variation of saturation temperature of isooctane with system pressure is given in Table 2.

Parameter	Range
Working fluid	Isooctane
System pressure	0.4 – 1 bar absolute
Injector tip temperature	60 – 170 $^{\circ}$ C
Air velocity	0 and 5 m/s
Air temperature	25 $^{\circ}$ C
Isooctane temperature	25 $^{\circ}$ C

Table 1. Experimental parameter range for the study.

A typical snapshot of the recorded event is shown in figure 4. Figure 4a and 4b show the IR images of the dry and wet injector tip, respectively. The IR intensity was not calibrated against the film or surface temperature. Residues left during soldering

resulted in variation in the tip emissivity, which resulted in the variation of IR intensity in figure 4a. The difference of these two images is shown in figure 4c, where the wetted state of the injector tip can be clearly identified.

Pressure, bar absolute	Saturation temperature, $^{\circ}$ C
0.4	69.6
0.6	81.9
0.8	91.2
1	98.9

Table 2. Saturation properties of isooctane [6].

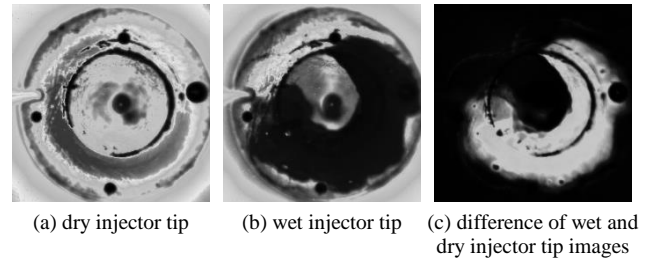


Figure 4. A typical snapshot of the recorded event.

Results and Discussion

At each experimental condition, 30 measurements were performed. A typical variation of drying time during a sequence of measurement is shown in figure 5. The scatter in the data is due to variability in the injection behaviour of the pump, which results in variation in the film spread area on the injector tip surface. Ideally, the air before the droplet injection is expected to be devoid of any isooctane vapour. To achieve this, fresh air was inducted into the test section are every few evaporation event. However, some vapour build-up between these induction events is expected, which may have additionally led to the scatter in the experimental data. The arithmetic mean of these 30 measurements is chosen as the representative drying time.

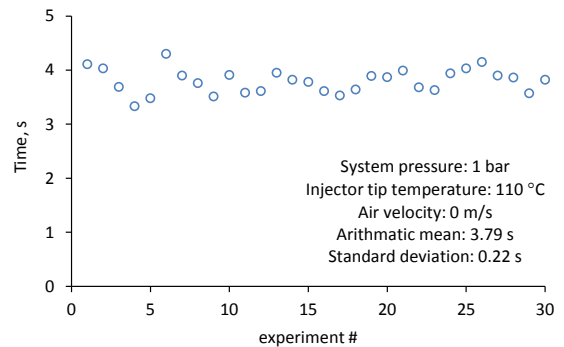


Figure 5. Variation of drying time during a measurement sequence.

Figure 6 shows the variation of drying time and the corresponding drying rate with injector tip temperature in quiescent air at 1 bar absolute. At 1 bar, the saturation temperature of isooctane is 98.9 $^{\circ}$ C. Up to an injector tip temperature of 110 $^{\circ}$ C (i.e. a superheat of 11.1 $^{\circ}$ C), the drying rate is low and the principle mode of drying is by evaporation at the three phase contact line [4,9]. The evaporation in still atmosphere is due to the combined effects of vapour phase natural convection and diffusion. The molecular weight of the isooctane is higher as compared to air by a factor of 3.9, which over the expected range of vapour temperature near the droplet would always result in the vapour being denser than the air. This should lead to a buoyancy-induced flow directed down and radially away from the surface of the drop. The drying rate during this evaporation dominated regime increases with the injector tip temperature. Beyond 110 $^{\circ}$ C, boiling started to occur

in the fuel film, with clearly seen bubbles or funnel-shaped structures [2] formation and bursting events (see Figure 7). The drying rate steeply increases with the incipience of boiling in the fuel film. At an injector tip temperature of 150 °C, boiling resulted in splashing of the fuel film away from the surface and the maximum drying rate was reached. At a wall temperature of 170 °C, the injected fuel bounced-off the injector tip during the injection event, which means that the Leidenfrost state is reached. However, the Leidenfrost temperature in the present study is slightly lower than that reported in drop impact studies of Stanglmaier et al. [10]. On the other hand, the temperature for achieving maximum vaporization rate was reported to be 122 °C, which is much lower than the finding of the present study.

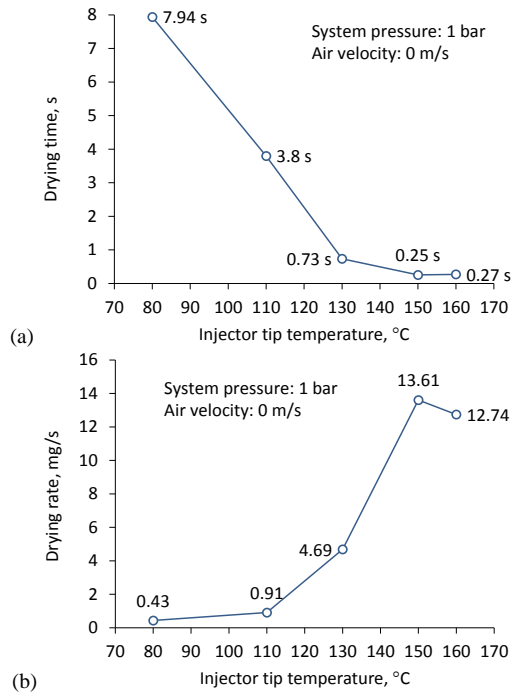


Figure 6. Variation of (a) drying time and (b) drying rate with injector tip temperature in quiescent air at 1 bar absolute.

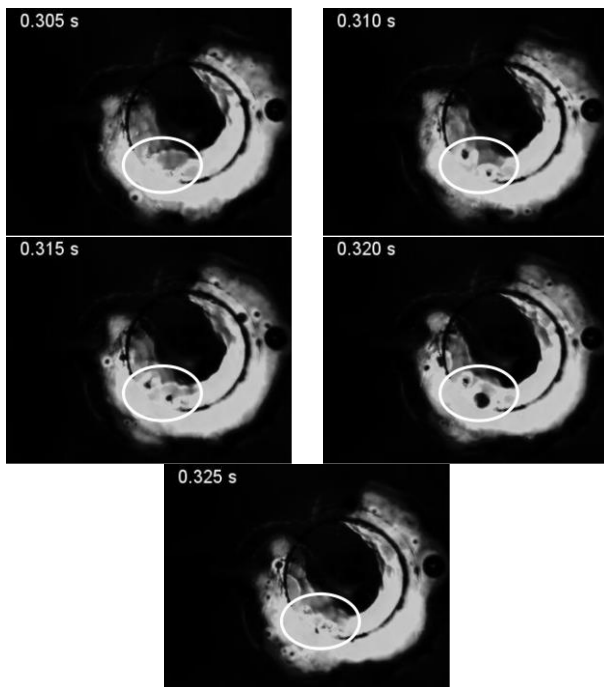


Figure 7. Sequence of images showing the bubble formation, growth and rupture events (1 bar absolute and injector tip temperature of 130 °C).

Figure 8 shows the variation of drying rate with injector tip temperature at various system pressures in quiescent air. As the saturation temperature reduces with system pressure, boiling within the film happens at lower injector tip temperature. The Leidenfrost temperature also reduces with system pressure. At the same injector tip temperature, the drying rate increases with reduction in system pressure. However, when compared at the same injector tip superheat, the drying rate decreases with reduction in system pressure. It is also found that the evaporation rate shows little dependence on the system pressure when compared at the same injector tip superheat. Interestingly, the maximum drying rate is reached at an injector tip superheat of 40 °C at all system pressure.

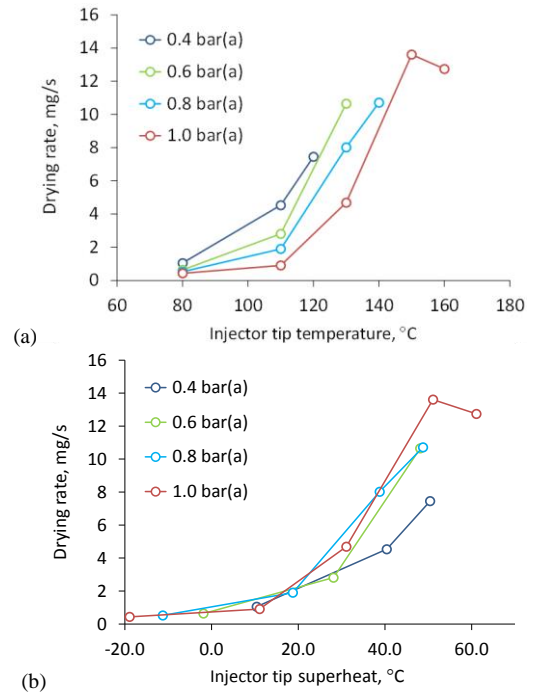


Figure 8. Variation of drying rate with (a) injector tip temperature and (b) superheat at various system pressures in a quiescent atmosphere.

Experiments with air flow were done only at one condition: system pressure of 0.8 bar absolute and air velocity of 5 m/s. The variation of system pressure and flow velocity in the test section is shown in figure 9. The variation of drying time and rate with injector tip temperature and the effect of air flow is shown in figure 10. It can be seen in that when the injector tip temperature is lower than the saturation temperature and evaporation is the dominating drying mechanism, the drying rate improves due to air flow. This enhancement is definitely due to the improvement in the mass transfer coefficient. However, when drying happens due to boiling, the drying rate does not increase due to air flow.

Conclusions

Generic experiments have been performed to understand the drying mechanism of the retained fuel film (isooctane in the present study) on the GDI injector tip. Based on this study, the following conclusions can be drawn:

- (i) Depending on the injector tip superheat, the drying out process can be dominated by either evaporation or boiling.
- (ii) At injector tip superheat up to 10 °C, evaporation is the dominating mechanism. The drying rate in this regime increases with injector tip temperature and air velocity but shows little dependence on the system pressure.
- (iii) The drying rate due to boiling depends on the system pressure and temperature but shows little dependence on the air velocity. Comparing at the same injector tip temperature,

the drying rate increases with the reduction in system pressure. However, at the same injector tip superheat, it reduces with system pressure.

(iv) The Leidenfrost temperature reduces with system pressure.

Future studies must focus on performing investigations with gasoline to determine the appropriate injector tip temperature for quick evaporation.

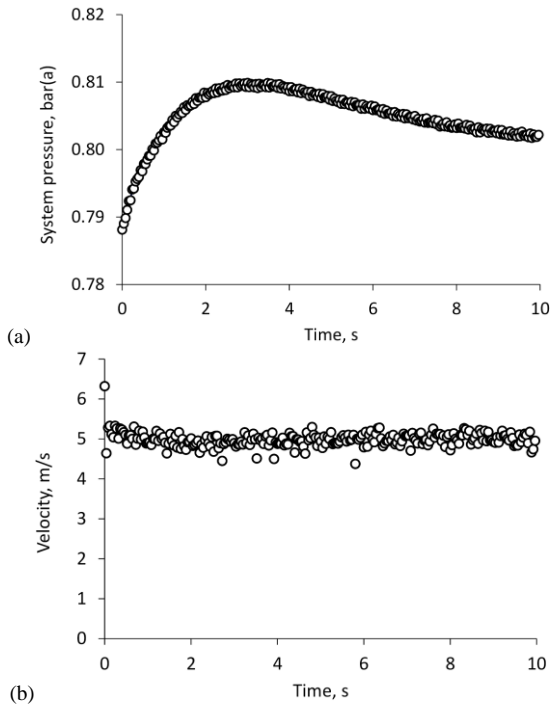


Figure 9. Variation of (a) system pressure and (a) air velocity in the test section with time on opening the inlet solenoid valve to the channel.

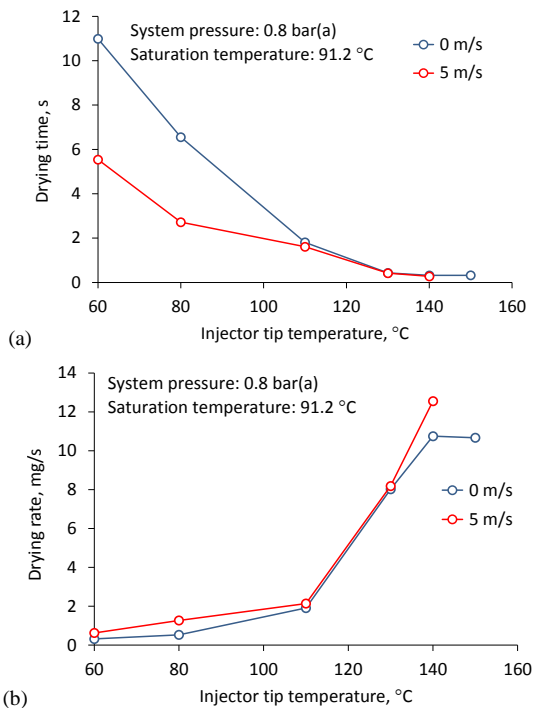


Figure 10. Effect of air flow on (a) drying rate and (b) drying time.

References

- [1] Berndorfer, A., Breuer, S., Piock, W. & Von Bacho, P., Diffusion Combustion Phenomena in GDI Engines caused by Injection Process, *SAE Tech. Pap.*, **2013-01-0261**, 2013.
- [2] Dorokhov, A.R. & Zhukov, V.I., Bubble growth rate and phenomenon of degenerate boiling of a fluid in the form of film vaporization, *J. Eng. Phys. Thermophys.*, **72(3)**, 1999, 430-437.
- [3] Heywood, J.B., *Internal Combustion Engine Fundamentals*, McGraw-Hill, 1988.
- [4] Ibrahim, K., Abd Rabbo, M.F., Gambaryan-Roisman, T. & Stephan, P., Experimental investigation of evaporative heat transfer characteristics at the 3-phase contact line, *Exp. Therm Fluid Sci.*, **34(8)**, 2010, 1036-1041.
- [5] Imoehl, W.J., Method of optimizing direct injector tip position in a homogeneous charge engine for minimum injector deposits, US Patent **6832593 B2**, 2004.
- [6] Linstrom, P.J. & Mallard, W.G (editors), NIST Chemistry WebBook, NIST Standard Reference Database Number 69, NIST, Gaithersburg MD, 20899, <http://webbook.nist.gov>, (retrieved July 10, 2014).
- [7] Oh, C., Considerations on influencing factors of carbon deposit in gasoline direct injection engine, *Proc. FISITA 2012 World Automotive Cong.*, Vol. 2: Advanced Internal Combustion Engines (II), Springer, 2013, 1369-1378.
- [8] Piock, W., Hoffmann, G., Berndorfer, A., Salemi, P. & Fushoeller, B., Strategies towards meeting future particulate matter emission requirements in homogeneous gasoline direct injection engines, *SAE Int. J. Engines*, **4(1)**, 2011, 1455-1468.
- [9] Plawsky, J.L., Ojha, M., Chatterjee, A. & Wayner, P.C., Review of the effects of surface topography, surface chemistry, and fluid physics on evaporation at the contact line, *Chem. Eng. Commun.*, **196(5)**, 2008, 658-696.
- [10] Stanglmaier, R., Roberts, C., & Moses, C., Vaporization of Individual Fuel Drops on a Heated Surface: A Study of Fuel-Wall Interactions within Direct-Injected Gasoline (DIG) Engines, *SAE Tech. Pap.*, **2002-01-0838**, 2002.
- [11] Stepien, Z. & Oleksiak, S., Deposit Forming Tendency In Spark Ignition Engines and Evaluation of Gasoline Detergent Additives Effectiveness, *J. KONES Powertrain Transport*, **16(2)**, 2009, 421-431.
- [12] Zhao, F., Lai, M.-C. & Harrington, D.L., Automotive spark-ignited direct-injection gasoline engines, *Prog. Energy Combust. Sci.*, **25**, 1999, 437-562.